Journal of the European Ceramic Society 20 (2000) 2407–2413

Sintering of tin oxide processed by slip casting

Iêda Maria Garcia dos Santos [a,*], Elson Longo [a], José Arana Varela [b], Edson Roberto Leite [a]

[a] *LIEC, Chemistry Department, UFSCar, Rod. Washington Luis, km 235, CP 676, cep 13565-905, São Carlos, SP, Brazil*
[b] *Universidade Estadual Paulista, Chemistry Institute, r. Prof. Francisco Degni, s/n, cep 14800-900, Araraquara, SP, Brazil*

Received 29 September 1999; received in revised form 1 May 2000; accepted 14 May 2000

Abstract

Sintering of SnO_2 compacts, obtained through slip casting, was studied by means of dilatometry, Hg porosimetry, scanning electron microscopy, and density measurement (Archimedes method). Sintering is strongly influenced by the green microstructure. Moreover, the sintering mechanisms are not dependent on the slurries' solid content up to 50% of solids in volume. Above this value, agglomerates are formed, leading to differential sintering inside and among the agglomerates. Another important point is the reduction of the temperature of maximum shrinkage rate when compared to tin oxide processed by isostatic pressing. This reduction is more accentuated when ammonium hydroxide is added to the suspension.

Keywords: Microstructure-final; Porosimetry; Sintering; Slip casting; SnO_2

1. Introduction

In modern ceramic science, the processing stage is considered fundamental to achieve densities close to the theoretical ones, fine microstructures and high mechanical properties.[1] In recent years, much effort has been made to increase the homogeneity of the green compact microstructure. Thus, powders having narrow particle size distribution and colloidal processing techniques have received special attention.[2]

When dealing with colloidal slurries, it has been observed that, if there are appropriate repulsive forces among the particles, they can slide over each other to form a uniform structure before becoming rigid. A poorly dispersed system or a flocculated slurry generates large spaces during consolidation.[2] Moreover, repulsive forces among the particles are used to separate weak agglomerates, to divide inclusions larger than a given size and to mix powders.[3]

Two conventional methods of slurry consolidation, slip casting and tape casting, can be used directly with powders prepared colloidally and, with a few modifications, injection molding can also be accomplished. Each of these conventional methods of casting is limited. Slip casting, for example, is more efficient in the casting of bodies with fine walls.[3] Moreover, due to its simplicity, slip casting is commonly used industrially.

The casting process can also be seen as a filtering process under pressure, the only difference being the dewatering process. In slip casting, suction pressure caused by capillary forces in a porous mold removes the liquid. Plaster of Paris molds have a suction pressure ranging from 0.1 to 0.2 MPa. Particle segregation during filtering may occur since fine particles can migrate through the pie and stop at the pie-mold interface if those particles are larger than the pores of the mold.[4] When this segregation occurs, the pie divides itself in two different areas. The area close to the mold presents a high concentration of small particles, while the ratio between the small particles and the large particles in the other area is the same as in the slurry. This process leads to a pie with variable density according to the thickness, and can influence the densifying behavior.[5]

A study was made of the sintering process of 0.5 mol% of manganese oxide-doped tin oxide[6] obtained by slip casting. This kind of material has a promising future, as these crucibles present resistance to corrosion by aggressive systems such as $YBa_2Cu_3O_7$ super-

* Corresponding author. Tel.: +55-16-261-5215; fax: +55-16-261-5215.
E-mail address: pigs@power.ufscar.br (I. Maria Garcia dos Santos).

0955-2219/00/$ - see front matter
PII: S0955-2219(00)00130-8

conductors and glasses containing heavy metal oxides and fluorides, which are usually processed in gold or platinum crucibles.[7–9]

2. Experimental procedure

The suspension was prepared by mixed oxide route, using a crystalline SnO_2 powder (Cesbra, Brazil) and 0.5 mol% of MnO_2 (Aldrich, USA) as dopant. The main characteristics of tin oxide are a surface area of 5.4 m^2/g with a mean particle size of 0.16 μm. The dispersing agent used was ammonium polyacrilate (PAA) (IQA-PAC C, IQA, Brazil) and the solvent used was distilled water.

Slurries containing different solid contents were milled in an attritor mill (01-HD, Union Process) for 0.5 hours at 500 rpm. Alumina balls with 2 mm of diameter were used as grinding media. The quantity of dispersant in the different slurries was optimized through the addition of small amounts of dispersant, followed by viscosity measurements. The best amount was the one that resulted in the lowest viscosity. The pH was optimized in the same way. Small amounts of ammonium hydroxide (Synth, Brazil) were added to the slurry, followed by a viscosity measurement. After optimization, six different slurries were prepared, as shown in Table 1.

Cylindrical pellets with 10 mm of diameter and 2 mm of height were formed by slip casting in plaster of Paris molds. After casting, the crucibles were dried at 100°C for 12 h. The pellets were characterized by scanning electron microscopy (SEM) (DSM 940, Zeiss) and Hg porosimetry (9310, Micromeritics). The latter test was carried out after calcining at 500°C for 1.5 h. Dilatometry (402EF, Netzch) of the cast bodies was also carried out after polishing to obtain pellets with parallel faces and a thickness of about 2 mm. The heating rate used was 10°C/min and the maximum temperature was 1500°C.

The sintered samples were characterized by Archimedes density measurements (in distilled water) and by SEM. The samples for SEM were cut transversally, polished and their grain boundaries revealed by thermal etching.

3. Results and discussion

The deflocculant of the slurries was optimized by viscosity measurements after adding small amounts of PAA. The optimization curves are shown in Fig. 1. After optimization, the pH of the slurries with higher solid contents (44.9 and 56.4 vol.%) was also optimized.

Micrographies obtained from green bodies showed that all the samples presented a small fraction of agglomerates, as indicated in Fig. 2. This demonstrates that the dispersion process was not entirely effective in eliminating the agglomerates, which are present in the starting material.

The green density measured by Hg porosimetry shows that density increases with the solid content of slurry, with a correlation coefficient (r) of 0.96, as illustrated in Fig. 3. This fact is explained by the small amount of water eliminated during the casting and drying processes. An important point is the increased dispersion obtained by adjustment of the pH, which leads to increased green density.

The pore size distribution curves (Fig. 4) show that all the cast samples presented a monomodal distribution, with average pore diameters ranging from 0.05 to 0.11 μm. Considering the mean particle size, all pores are smaller than it. This fact is quite significant since small pores with a low coordination number are thermodynamically unstable and can easily be eliminated during the sintering process.[10]

The values of the most frequent pore diameter and the dispersion around this value, represented by the full width to half maximum (FWHM), are illustrated in Table 2. It can be observed that the increased concentration of solids in the slurries leads to a continuous decrease of the most frequent pore diameter. A similar behavior was observed for the FWHM. Hence, it is expected that samples molded from more concentrated slurries will reach a higher densification level, since smaller pores are easier to eliminate.

The adjustment of the pH also leads to a decrease in the most frequent pore diameter, but does not change the FWHM. The increased content of solids in slurries containing over 50 vol.% of solids does not change the pore structure.

Table 1
Slurries used in the casting of crucibles

Slurry	Dispersant (wt.%)	Solid content (vol.%)	Optimization of pH
1	0.30	17.7	–
2	0.20	25.1	–
3	0.15	36.5	–
4	0.16	44.9	–
5	0.16	44.9	9.23
6	0.16	56.4	9.92

Table 2
Data obtained from Hg porosimetry

Solid content (%)	Diameter of the most frequent pore (μm)	FWHM (μm)
17.7	0.093±0.001	0.037±0.002
25.1	0.078±0.001	0.023±0.001
36.5	0.074±0.001	0.023±0.003
44.9	0.063±0.001	0.021±0.001
44.9 (pH adjustment)	0.052±0.001	0.020±0.001
56.4 (pH adjustment)	0.051±0.001	0.022±0.001

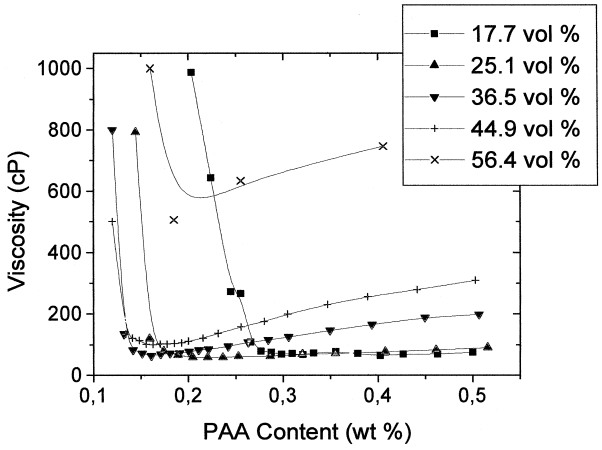

Fig. 1. Viscosity of slurries as function of the PAA content and the solid content.

Fig. 5 presents a linear shrinkage curve, characteristic of the materials used in the present work. From linear shrinkage curves and green density results, densification rate was calculated, according to Eqs. (1) and (2).

$$D = \frac{D_0}{[1 + \Delta L/L_0]^3}, \tag{1}$$

$$\frac{dD}{dT} = \frac{-3D_0}{[1 + \Delta L/L_0]^4} \times \frac{d(\Delta L/L_0)}{dT}, \tag{2}$$

where D is the relative density, D_o is the relative green density, $\Delta L/L_o$ is the relative linear shrinkage, T is the temperature, dD/dT is the densification rate, and $d(\Delta L/L_o)/dT$ is the linear shrinkage rate.

The results shown in Fig. 6a and b indicate that the densification rate and relative density are controlled by the green microstructure. Samples with low green density (Fig. 6a), obtained from less concentrated slurries dispersed with PAA, present a higher densification rate at a lower relative density. Samples with higher green density (Fig. 6b) present a maximum densification rate at a higher relative density.

The curve symmetry is an important factor to observe. Lange[11] suggests that the densifying mechanisms control sintering up to a maximum of the densification rate and that, at densities above this value, sintering is controlled by non-densifying mechanisms such as grain growth. It follows, therefore, that the high symmetry (observed in the curves for the samples cast from slurries containing 17.7 to 44.9 vol.%, with and without the addition of ammonium hydroxide) indicates that the densifying mechanisms and grain growth act differently, with a rapid change from one mechanism to another, as the temperature increases. This result is in agreement with the study of Cerri et al.[6] for SnO_2 samples doped with 0.5 mol% of MnO_2 and obtained by isostatic pressing. This means that, in the present case (except for slurries with added ammonium hydroxide), sintering mechanisms do not depend on powder processing.

According to Roosen et al.[2] the elimination of small pores inside the agglomerates is reflected to a maximum in the densification rate curves at low temperatures. Larger pores among the agglomerates require higher temperatures for their elimination. This differential shrinkage due to agglomerates leads to the presence of a second peak in the derivative curve of linear shrinkage vs. temperature. The plots presented in Fig. 6b also reflect this behavior, as the densification rate is

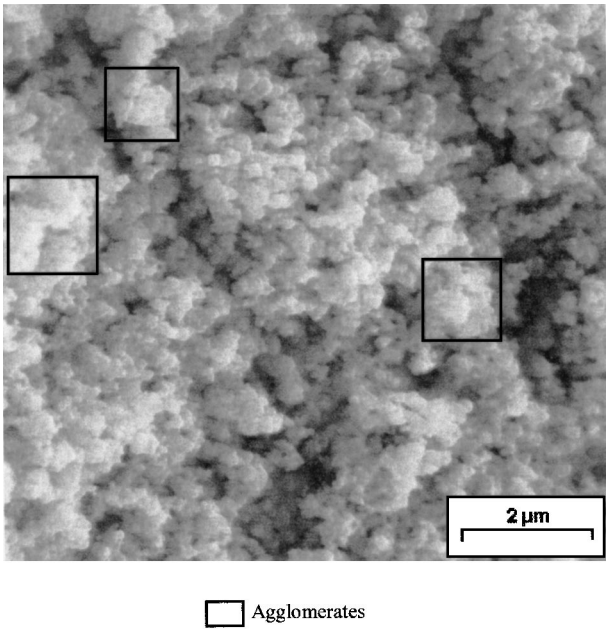

Fig. 2. SEM micrograph before sintering showing presence of agglomerates.

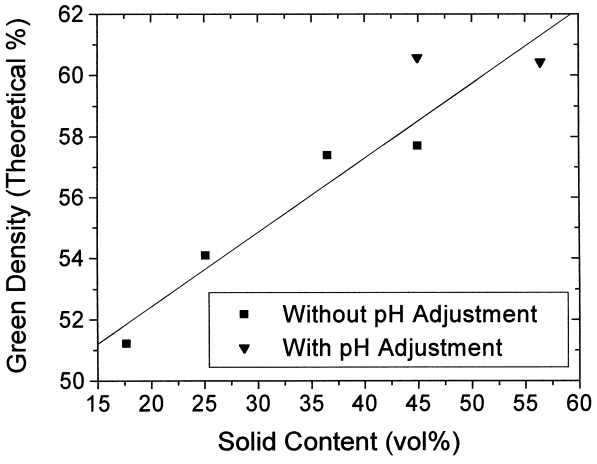

Fig. 3. Variation of green density as a function of the solid content (SnO_2 theoretical density is 6.95 g/cm^3).

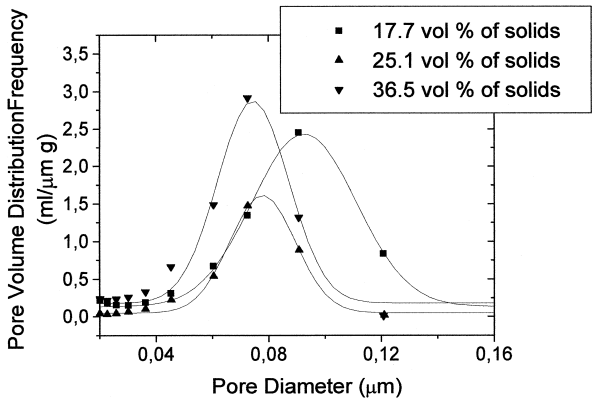

(a)

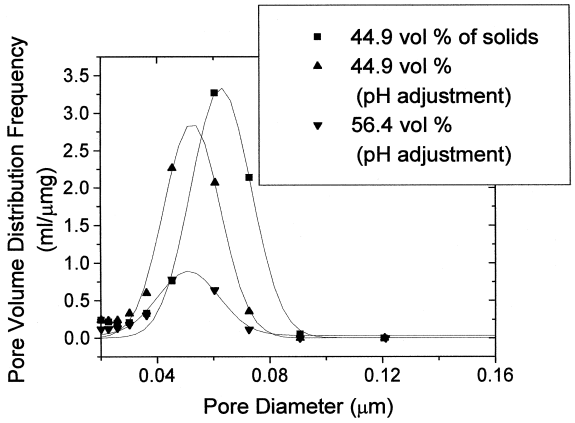

(b)

Fig. 4. Graph showing pore size distribution frequency (dV/dD) as a function of the pore diameter and of the solid content.

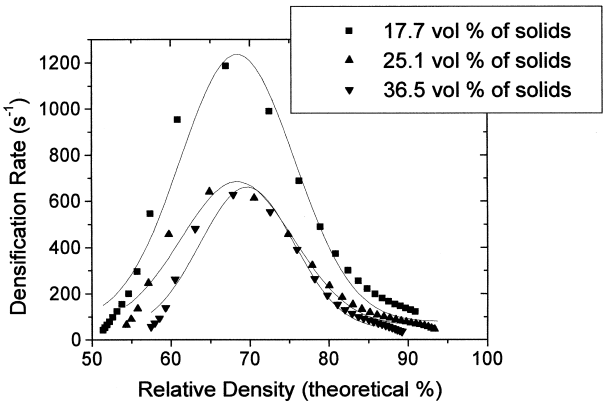

(a)

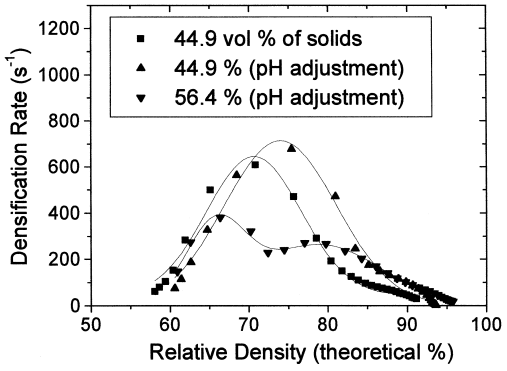

(b)

Fig. 6. Variation of the densification rate as a function of the relative density and of the solid content.

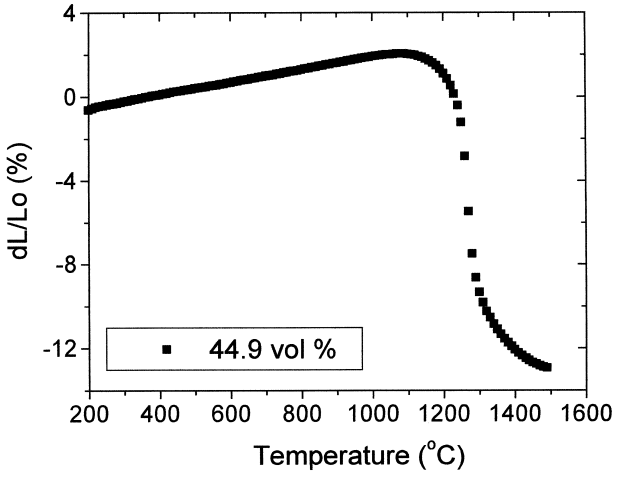

Fig. 5. Graph showing length change vs temperature for pellet casted from suspension containing 44.9 vol.% of solids.

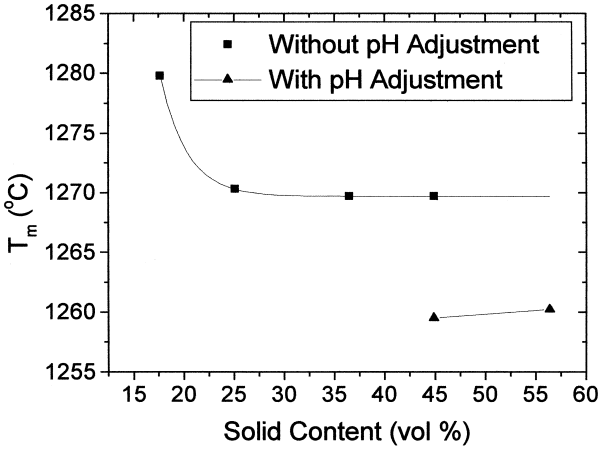

Fig. 7. Variation of the temperature of maximum shrinkage rate (T_m), as a function of the solid content.

calculated from the linear shrinkage curve as a function of temperature.

This second peak was not observed in the samples cast from slurries with concentrations of solids below 50 vol.%, indicating that the agglomerates observed by SEM do not alter the sintering mechanism. This sintering behavior, without differential densification rate, is due to the small fraction of agglomerates.

Two peaks are observed in the samples cast from slurries with a 56.4 vol.% concentration of solids, indicating

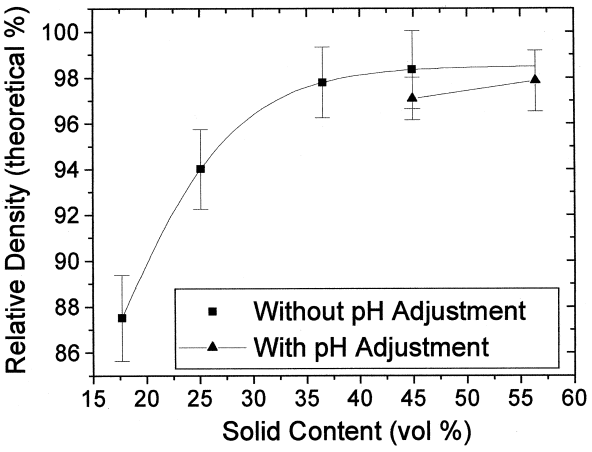

Fig. 8. Density after sintering as a function of the solid content.

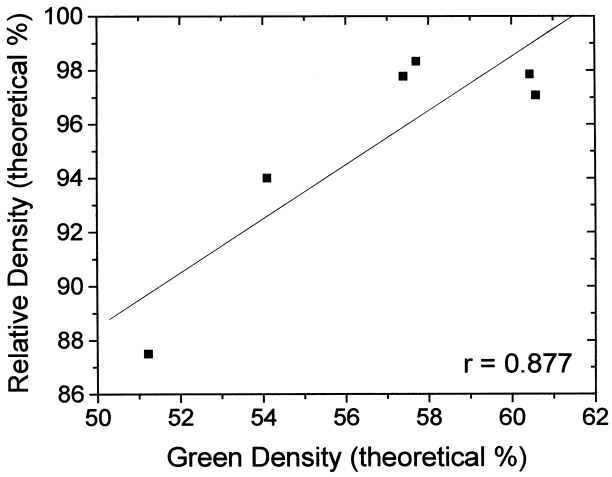

Fig. 9. Sintered density as a function of green density.

that differential sintering of agglomerates occurs. This effect is due to the high concentration of solids, which makes system dispersion more difficult since the particles are very close. According to Pugh et al.[4] when the concentration of solids exceeds 54 vol.%, the suspension is fully crystallized. It is important to emphasize that the sample with 44.9 vol.%, which had its pH adjusted, did not present this second peak.

The temperature of maximum shrinkage rate (T_m) was obtained from the differential curves of shrinkage as a function of the temperature, as shown in Fig. 7. A comparison with the results of Cerri et al.[6] ($T_m = 1280°C$) indicates that colloidal processing leads to a small decrease of this temperature when a higher content of solids in the slurries is used. According to Roosen et al.[2] during colloidal conformation, the powder surface may be changed by hydrolysis, which leads to a change in the particles' interface. This hydrolysis may lead to the formation of cemented contact points that favors densification and may also be responsible for grain growth.

In this case, it was observed that, at a low solids content (17.7 vol.%), the T_m was higher due to the low packing of the particles. Another significant factor was that, when ammonium hydroxide was added, the T_m was significantly reduced. This was probably due to the defect formation, which plays an important role in the sintering of tin oxide. The elimination of hydroxyls adsorbed on the particles' surface leads to the formation of oxygen defects, which favor densification and consequently reduce T_m. When ammonium hydroxide is added, the higher basicity of ammonia leads to the formation of a larger number of defects and, hence, to a greater reduction of T_m. It is important to emphasize that tin oxide is chemically stable in pH 9.9.

Fig. 8 illustrates the relationship between the density after sintering at 1285°C for 4 h and the concentration of solids in the slurry. It can be observed that samples obtained from more concentrated slurries presented higher densities after sintering. The highest density (~98%) was obtained for sample cast from slurry with concentration of solids above 36.5 vol.%.

The density of the sintered samples was compared to the green density (Fig. 9), to the FWHM and to the diameter of the most frequent pore. The correlation coefficient ($r = 0.877$) indicates that the density after sintering is related to the green density, but no relation with FWHM and with the most frequent pore diameter was found.

An important point is that samples casted from suspensions in which the pH was adjusted did not present the highest density after sintering, in spite of the highest green density. To explain this fact, it is postulated that the ammonium hydroxide addition can modify the surface of SnO_2 particles, which can modify sintering process, decreasing the T_m. As consequence, an increase in the grain growth rate must occur. Thus, a lower density after sintering was obtained.

Fig. 10 presents the micrographies after sintering at 1285°C. The reduction of porosity with the increased concentration of solids in the slurries can be observed, confirming the data presented in Fig. 8. The samples cast from slurries with 17.7 vol.% (Fig. 10a) and 25.1% of solids (Fig. 10b) present a high porosity, with longer time or higher temperature for pore elimination being required. Samples with 36.5 vol.% of solids (Fig. 10c) and with 44.9 vol.% of solids (Fig. 10d) are quite dense.

An important point is the increased grain size of the samples cast from slurries that received additions of ammonium hydroxide (compare Fig. 10d and e). As explained above, this fact may be due to the smaller T_m of these samples and to a sintering mechanism that favors grain growth. As all the samples were sintered at the same temperature (1285°C) and for the same length of time, grain growth was favored in the samples exhibiting lower T_m. The larger grain size distribution in the sample molded from the slurries containing 56.4

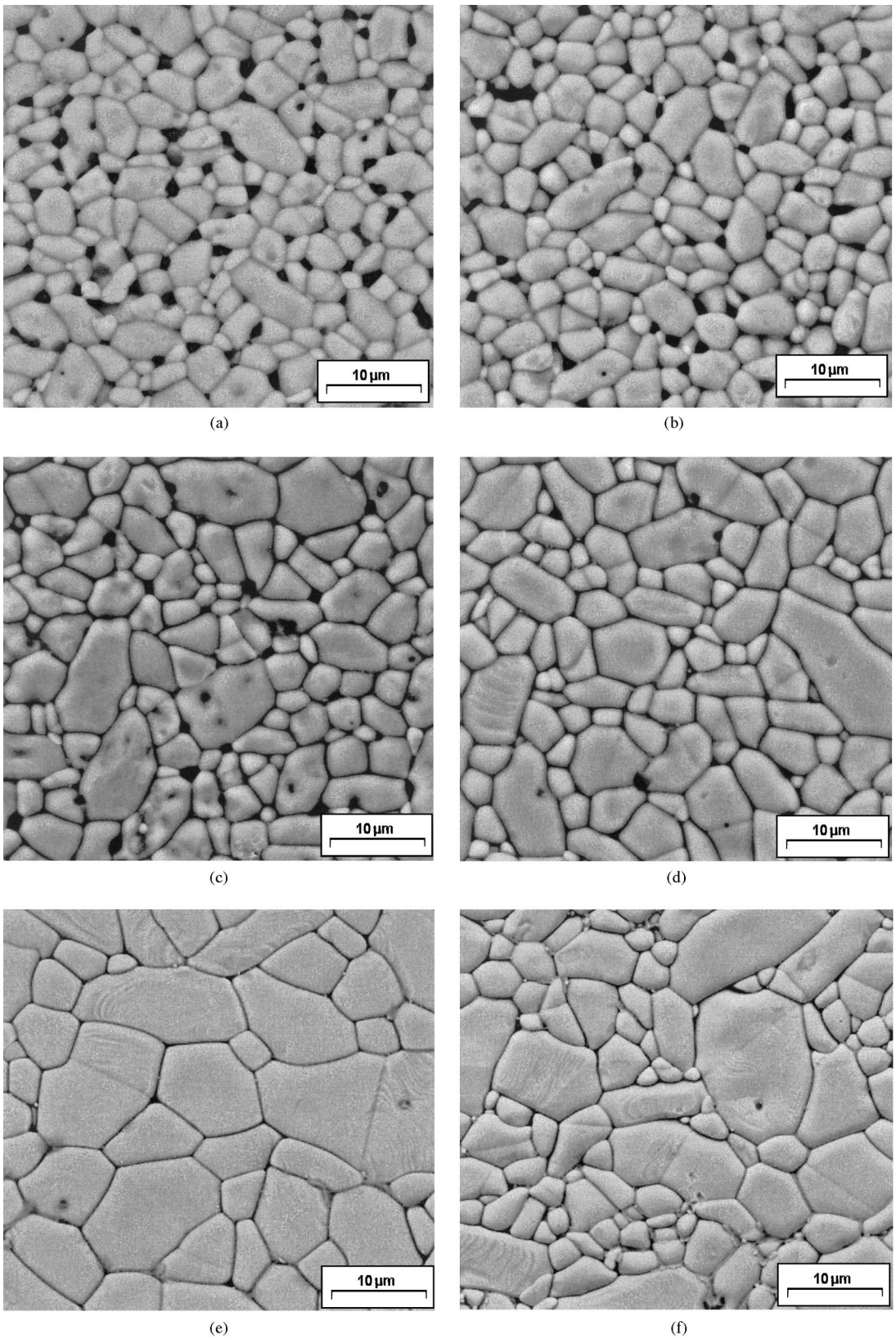

Fig. 10. Micrographies showing microstructures of the samples sintered at 1285°C for 4 h. (a) 17.7 vol.%; (b) 25.1 vol.%; (c) 36.5 vol.%; (d) 44.9 vol.%; (e) 44.9 vol.%, with pH adjustment; (f) 56.4 vol.% with pH adjustment.

vol.% (Fig. 10f) may be due to the presence of agglomerates, which led to differential sintering, as illustrated in Fig. 6b.

4. Conclusions

From the results obtained, it may be concluded that sintering of tin oxide doped with 0.5 mol% of manganese oxide is strongly influenced by the green microstructure. Samples cast from more concentrated slurries present a higher green density, narrower pore size distribution and, after sintering, a higher density. Slurries with concentrations of solids above 50 vol.% lead to the formation of compacts with agglomerates that sinter differentially. A comparison with the results obtained by Cerri et al.[6] indicates that sintering mechanisms do not depend on the processing used in the powder conformation when the concentration of dopant is the same. On the other hand, hydrolysis on the powder's surface leads to the formation of contact points among the particles, leading to the reduction of T_m and a change in the sintering mechanism.

Acknowledgements

The authors gratefully acknowledge the financial support of the Brazilian financing institutions FAPESP, MCT/PRONEX and FINEP/PADCT for this work, and IQA (Brazil) for supply of the dispersant.

References

1. Moreno, R., Moya, J. S. and Requena, J., Colaje de oxidos ceramicos I: fundamentos. *Bol. Soc. Esp. Ceram. Vidr*, 1985, **24**, 165–171.
2. Roosen, A. and Bowen, H. K., Influence of various consolidation techniques on the green microstructure and sintering behavior of alumina powders. *J. Am. Ceram. Soc.*, 1988, **71**, 970–977.
3. Lange, F. F., Powder processing science and technology for increased reliability. *J. Am. Ceram. Soc.*, 1989, **72**, 3–15.
4. Pugh, R. J. and Bergströn, L., *Surface and Colloid Chemistry in Advanced Ceramic Processing*. Marcel Dekker, Inc., New York, 1994 pp. 204–208, 279–281.
5. Hampton, J. H. D., Savage, S. B. and Drew, R. A. L., Experimental analysis and modeling of slip casting. *J. Am. Ceram. Soc.*, 1988, **71**, 1040–1045.
6. Cerri, J. A., Leite, E. R., Gouvea, D., Longo, E. and Varela, J. A., Effect of Cobalt (II) Oxide and Manganese (IV) Oxide on Sintering of Tin (IV) Oxide. *J. Am. Ceram. Soc.*, 1996, **79**, 799–804.
7. Rojas-Ramírez, R. A., *Crescimento de Monocristais Supercondutores $YBa_2Cu_3O_7$ — Pelo Método de Fluxo em Cadinhos de SnO_2*; Masters thesis, Universidade Federal de São Carlos, Brasil, 1998.
8. Cerri, J. A., Santos, I. M. G., Longo, E., Leite, E. R., Lebullenger, R. M., Hernandes, A. C. and Varela, J. A., Characteristics of $PbO–BiO_{1.5}–GaO_{1.5}$ melted in SnO_2 crucibles. *J. Am. Ceram. Soc.*, 1998, **81**, 705–708.
9. Lebullenger, R., et al, SnO_2 ceramic crucible for fluoride glasses melting. *J. Non-Crystal Sol.*, Submitted for publication.
10. Hirata, Y., Nishimoto, A. and Ishihara, Y., Effects of addition of polyacrylic ammonium on colloidal processing of α-alumina. *J. Ceram. Soc. Japan*, 1992, **100**, 983–990.
11. Lange, F. F., Approach to reliable powder processing. In *Ceram. Trans., Vol. 1*, ed. G. L. Messing, E. R. Fuller Jr. and H. Hausner. American Ceramic Society, Westerville, OH, 1989, pp. 1069–1083.